Not Much Helicity is Needed to Drive Large Scale Dynamos

Jonathan Pietarila Graham[1], Eric G. Blackman[2], Pablo D. Mininni[3,4] and Annick Pouquet[3]
[1] *Solid Mechanics and Fluid Dynamics (T-3) & Center for Nonlinear Studies;*
Los Alamos National Laboratory MS-B258; Los Alamos NM 87545, U.S.A.
[2] *Department of Physics and Astronomy; University of Rochester; Rochester NY 14627; U.S.A.*
[3] *Computational and Information Systems Laboratory; NCAR; P.O. Box 3000, Boulder CO 80307-3000, U.S.A.*
[4] *Departamento de Física, Facultad de Ciencias Exactas y Naturales,*
Universidad de Buenos Aires & IFIBA, CONICET; Ciudad Universitaria, 1428 Buenos Aires, Argentina.
(Dated: March 26, 2018)

Understanding the in situ amplification of large scale magnetic fields in turbulent astrophysical rotators has been a core subject of dynamo theory. When turbulent velocities are helical, large scale dynamos that substantially amplify fields on scales that exceed the turbulent forcing scale arise, but the minimum sufficient fractional kinetic helicity $f_{h,C}$ has not been previously well quantified. Using direct numerical simulations for a simple helical dynamo, we show that $f_{h,C}$ decreases as the ratio of forcing to large scale wave numbers k_F/k_{min} increases. From the condition that a large scale helical dynamo must overcome the backreaction from any non-helical field on the large scales, we develop a theory that can explain the simulations. For $k_F/k_{min} \geq 8$ we find $f_{h,C} \lesssim 3\%$, implying that very small helicity fractions strongly influence magnetic spectra for even moderate scale separation.

Introduction The origin of magnetic fields in turbulent astrophysical rotators such as stars, galaxies [1] and accretion disks has been a long standing topic of research. A particular challenge has been to understand the origin of fields on scales that are large compared to those of any underlying turbulence [1–4].

That the large scale field of the sun reverses every 11 years reveals that such stellar fields cannot be simply the residual of flux freezing from the primordial material and must be amplified in situ. Complementarily, the continuous processing by supernovae driven turbulence in galaxies likely renders the role of any primordial fields to be simply seed fields whose in situ processing must be understood to account for the observed present day large scale fields in galaxies. The presence of astrophysical jets from accretion engines also highlights the presence of large scale fields in accretion disks, and accretion disk simulations [3] commonly show the in situ generation of large scale magnetic fields that reverse on cycle periods of tens of orbit times.

The study of in situ field amplification in the presence of velocity flows is the enterprise of dynamo theory. Small scale dynamos (SSDs), in which turbulent velocity flows amplify fields at or below scales of the forcing [5, 6], can be distinguished from large scale dynamos (LSDs) in which magnetic fields are amplified on spatial or temporal variation scales larger than the scales of the underlying forcing. LSDs and SSDs are often contemporaneous and interactive (see e.g. [4, 7]) but LSDs arise only when turbulent velocities are sufficiently helical [8, 9]. There has been little previous work, however, on determining the minimum sufficient helicity to incite LSD action and this is the topic of the present paper. Astrophysical flows are unlikely to be 100% helical in environments where LSDs are presumed; the galaxy for example is estimated to have helicity of < 10%. Thus the basic question of how much helicity is required in even the simplest LSDs is important in assessing the potential ubiquity of LSDs.

The standard 20th century textbook [10] kinematic approach to LSD theory has been classical mean field (MFT) which features the $\alpha-$effect: $\gamma = |\alpha|k - \beta k^2$, where γ is the exponential growth rate in the kinematic dynamo regime (presuming that any Lorentz-force feedback is negligible), k is the wavenumber of magnetic field growth, the $\alpha-$effect is proportional to kinetic helicity $H_v = \langle \mathbf{v} \cdot \boldsymbol{\omega} \rangle$, with $\mathbf{v}$ the velocity and $\omega = \nabla \times \mathbf{v}$ the vorticity, and β is the turbulent eddy diffusivity [10]. Such mean-field theory has been used to model solar [11], stellar, and galactic observations, as well as laboratory plasma dynamos [12], and Geo-dynamos [13].

But the kinematic approach to LSD theory is incomplete. Although many astrophysical rotators have differential rotation and open boundaries, substantial progress in going beyond the kinematic theory has emerged from studies of the closed volume "α^2" helical dynamo without shear, in which the evolution of an initially weak seed field is subject to helical velocity forcing. The α^2 dynamo was first tackled semi-analytically [9] using a spectral integro-differential model with an Eddy Damped Quasi-Normal Markovian (EDQNM) closure, consistently tracking the magnetic helicity. It was shown that the actual driver of large scale magnetic field growth is not just the kinetic helicity, but the residual helicity, $H_R = H_v - H_j$ where the current helicity $H_j = \langle \mathbf{j} \cdot \mathbf{b} \rangle$ and $\mathbf{j} = \nabla \times \mathbf{b}$ is the current density.

This α^2 dynamo in a periodic box was simulated [14] by forcing with kinetic helicity at wavenumber $k_F = 5k_{min}$ ($k_{min} = 1$ was the smallest wavenumber of the flow). The large-scale ($k < 5$) field grew as expected from Ref. [9]. Subsequently, a two-scale α^2 LSD was developed [15]; it incorporated magnetic helicity evolution using a simpler closure than EDQNM and showed even a two-scale nonlinear theory predicts the evolution and saturation of LSD growth observed in [14]. Driving with kinetic helicity initially produces a large scale helical magnetic field, but the near conservation of magnetic helicity leads to a compensating small scale magnetic (and current) helicity of opposite sign. This counteracts the kinetic helicity driving in the large scale field growth coefficient, and quenches the LSD, as proposed in [9].

There has also been a plethora of work on the SSD. In a periodic box with a weak initial seed field and non-helical forcing, the stochastic line stretching produces negligible field growth above the forcing scale. Simulations of non-helical SSDs without large scale shear show that the total magnetic energy is amplified to near equipartition with the total kinetic energy not only in the kinematic regime as predicted by [5], but also in the saturated regime for large magnetic Prandtl number $P_M = \nu/\eta$, where ν and η are the viscosity and magnetic diffusivity [6, 16, 17], as reviewed in [7]. Astrophysical plasmas such as the Galactic interstellar medium do not seem to exhibit this pile-up [18].

To address this disparity between simulations of non-helical SSDs and how conditions favorable for LSD growth might influence the magnetic spectrum on both large and small scales, results for dynamos in a periodic box forced with different amounts of fractional kinetic helicity f_h (a dimensionless measure of the degree of alignment between the velocity and the vorticity of the forcing function), were studied [19]. It was found that the magnetic spectrum above and below the forcing scale were contemporaneously affected by a sufficient f_h. The large scale field grew, and the magnetic spectrum at large wave numbers steepened. For $f_h = 1$ and $f_h = 0$, the results of [14] and [17] were respectively recovered.

But the restriction in [19] to a forcing scale of $k_F = 5$ and resolution of 64^3 grid points left key unexplored questions. In particular, the minimum f_h for LSD action, $f_{h,C}$, could not be determined as a function of k_F. The smaller this minimum, the potentially more ubiquitous LSD conditions are in astrophysics. Here we perform much higher resolution simulations for fractionally helical dynamos and quantify how $f_{h,C}$ depends on k_F/k_{min}. We also develop a theory that correctly predicts the dependence, seen in the simulations.

Equations and set-up- The incompressible MHD equations for velocity $\mathbf{v}$ and magnetic field $\mathbf{b}$ are:

$$\begin{aligned} \partial_t \mathbf{v} + \boldsymbol{\omega} \times \mathbf{v} &= \mathbf{j} \times \mathbf{b} - \boldsymbol{\nabla} p + \nu \nabla^2 \mathbf{v} + \mathbf{F} \\ \partial_t \mathbf{A} &= \mathbf{v} \times \mathbf{b} - \nabla \phi + \eta \nabla^2 \mathbf{A} \\ \boldsymbol{\nabla} \cdot \mathbf{v} &= 0 \, , \quad \boldsymbol{\nabla} \cdot \mathbf{A} = 0. \end{aligned} \tag{1}$$

The total pressure divided by the constant (unit) density p and the potential ϕ are obtained self-consistently to ensure incompressibility and the Coulomb gauge. The Reynolds number is $Re = U_{rms} L_0/\nu$, with U_{rms} and $L_0 = 2\pi \int E(k) k^{-1} dk / \int E(k) dk$ the r.m.s. velocity and the integral scale respectively; the magnetic Reynolds number is defined as $R_M = U_{rms} L_0/\eta$. In the following, E denotes the total energy, and E_v and E_b denote the kinetic and magnetic energy respectively.

We employ a well-tested pseudo-spectral code that uses a hybrid parallelization, combining Message Passing Interface (MPI) and OpenMP [20]. The computational box has size $[2\pi]^3$, and wave numbers vary from $k_{min} = 1$ to $k_{max} = N/3$ using a standard 2/3 de-aliasing rule, where N is the number of grid points per direction.

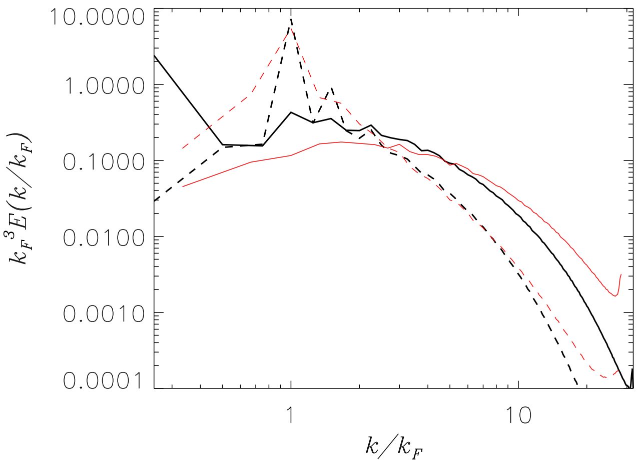

FIG. 1. (*Color online*) Re-dimensionalized magnetic (solid) and kinetic (dashed) energy spectra after 90τ for run 4-60 (thick) black forced at $k_F = 4$ and for run 3-60 (thin red/light gray) with $k_F = 3$. At a fixed $f_h = 60\%$ here, increased scale separation provides for the transition between SSD and LSD.

The forcing applied at k_F is $\mathbf{F} \equiv \mathbf{F}_R + c\mathbf{F}_A$; $\mathbf{F}_A$ is an ABC flow at k_F, and $\mathbf{F}_R$ is the sum of all harmonic modes with $k = k_F$ and random phases. We choose c for a given fractional helicity of $\mathbf{F}$, $|f_h| \leq 1$, with $f_h \equiv \langle \mathbf{F} \cdot \boldsymbol{\omega}_{\mathbf{F}} \rangle (\langle |\mathbf{F}|^2 \rangle \langle |\boldsymbol{\omega}_{\mathbf{F}}|^2 \rangle)^{-1/2}$, where $\omega_F = \nabla \times \mathbf{F}$. The entire forcing has random phases applied, with a correlation time $t_{cor} = 0.1$. In practice, the ratio of helical to non-helical forcing magnitudes is $c \simeq [f_h/(1-f_h)]^{1/2} \equiv R_h$. The kinetic helicity at k_F is typically within 25% of f_h. By choosing dimensional length and time constants $l_0 \propto k_F$ and t_0 (fixed), varying k_F in our simulations corresponds to dimensionalized physical systems described by Eqs. (1), where the forcing scale is constant and the system size increases $\propto k_F$. The dimensionless velocity v_{rms} and forcing are $\propto k_F^{-1}$, and the diffusivity $\propto k_F^{-2}$.

A hydrodynamic state is evolved for five forcing-scale eddy turnover times, τ, before a magnetic seed field at $k = k_{seed}$ is introduced. In the hydro steady state, the resulting $\tau = 2\pi [k_F U_{rms}]^{-1} \approx 4.2$. In all simulations, dimensionalized viscosity is constant, $k_F^2 \nu = 2.412 \cdot 10^{-2}$, and, arbitrarily, $P_M = 4$ so that $P_M > 1$ while limiting the computational cost (see Table I for further details).

Simulation Results- Table I summarizes our runs. The kinetic and magnetic energy spectra after $t = 90\tau$ are displayed in Fig. 1, for runs 4-60 (with $k_F = 4$) and 3-60 (with $k_F = 3$). Both have f_h=60%, and for both, the small-scale fields grow; only for $k_F = 4$ does $k = 1$ grow.

Figure 2 shows the growth of magnetic energy in the $k = 1$, $k = 6$, and total over all modes for run 3-80. The evolution exhibits an early phase in which both modes grow at the same rapid rate, with $\gamma_{SSD} \sim 0.33 \sim \tau^{-1}$, followed by a slow growth of the $k = 1$ mode and a sat-

TABLE I. Parameters: Runs are labeled by the forcing wavenumber k_F followed by the percentage of helicity in the forcing f_h; R_M and k_{seed} are defined in the text ($Re = R_M/4$). The SSD growth rate is γ_{SSD}. E_b^s is the magnetic energy and H_b is the magnetic helicity, both at later times, between 60τ and 130τ; the "f" is for fluctuating, and "g" is for growing exponentially (indicating a helical dynamo). Forcing wave numbers are $k_F = 2, 3, 4, 5, 6$ and 8 for runs on grids of $192^3, 256^3, 384^3, 432^3, 512^3$ and 768^3 points respectively. *Run 3-80 was pursued until $t \approx 300\tau$, at which time $E_b \sim 0.3$ and $H_b \sim 10$. See Fig. 2.

Run	R_M	k_{seed}	γ_{SSD}	$\gamma_{k=1}$	E_b^s	$-100H_b$
2-80	1500	[6.7,10.7]	0.24	$(-1.2 \pm 10)10^{-4}$	0.2	$0.5f$
2-85	1600	–	0.22	$(5.6 \pm 0.7)10^{-3}$	0.4	$6g$
2-90	1600	–	0.24	$(6.0 \pm 0.7)10^{-3}$	0.4	$8g$
3-40	2000	[10,16]	0.31	$(-1.0 \pm 7.6)10^{-4}$	0.1	$0.1f$
3-60	1900	–	0.32	$(3.7 \pm 7.3)10^{-4}$	0.1	$0.2f$
3-69	1700	–	0.27	$(6.0 \pm 0.7)10^{-3}$	0.1	$1.0g$
3-80	2000	–	0.33	$(8.6 \pm 1.4)10^{-3}$	0.3*	$10g^*$
4-10	1700	[13.3,21.3]	0.25	$(-1.6 \pm 2.0)10^{-3}$	0.04	$0.008f$
4-20	1600	–	0.28	$(5.9 \pm 0.6)10^{-3}$	0.04	$0.06g$
4-40	1600	–	0.25	$(1.5 \pm 0.1)10^{-2}$	0.06	$0.3g$
4-60	1500	–	0.25	$(2.8 \pm 0.2)10^{-2}$	0.1	$1.0g$
4-80	1600	–	0.27	$(2.8 \pm 0.3)10^{-2}$	0.1	$1.9g$
5-09	2000	[16.7,26.7]	0.26	$(5.9 \pm 4.5)10^{-4}$	0.03	$0.004f$
5-19	1900	–	0.26	$(-2.5 \pm 0.7)10^{-3}$	0.03	$0.007f$
5-40	1800	–	0.27	$(1.6 \pm 0.7)10^{-3}$	0.03	$0.03g$
5-50	1900	–	0.27	$(3.5 \pm 1.4)10^{-3}$	0.03	$0.06g$
5-60	1800	–	0.28	$(1.1 \pm 0.09)10^{-2}$	0.04	$0.3g$
6-01	1700	[20,32]	0.27	$(2.2 \pm 11)10^{-4}$	0.02	$0.002f$
6-05	1700	–	0.24	$(4.1 \pm 5.0)10^{-4}$	0.02	$0.003g$
6-10	1700	–	0.27	$(-1.5 \pm 6.9)10^{-4}$	0.02	$0.004g$
6-15	1600	–	0.23	$(1.1 \pm 0.7)10^{-3}$	0.02	$0.007g$
6-20	1700	–	0.27	$(4.5 \pm 2.0)10^{-3}$	0.03	$0.01g$
6-30	1600	–	0.23	$(3.6 \pm 0.9)10^{-3}$	0.03	$0.02g$
6-40	1600	–	0.23	$(7.4 \pm 0.7)10^{-3}$	0.03	$0.06g$
8-03	1200	[26.7,42.7]	0.20	$(5.4 \pm 1.9)10^{-3}$	0.008	$4 \cdot 10^{-4}g$

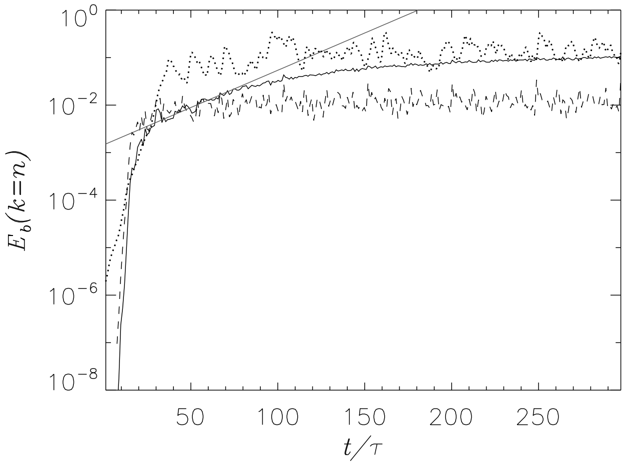

FIG. 2. Magnetic energy density $E_b(k)$ for $k = 1$ (solid line), $k = 6$ (dashed) and total (dotted) versus time for run 3-80. The gray line indicates the fit $\gamma = (8.6 \pm 1.4)10^{-3}$ to the solid curve for growth of the $k = 1$ mode after SSD saturation.

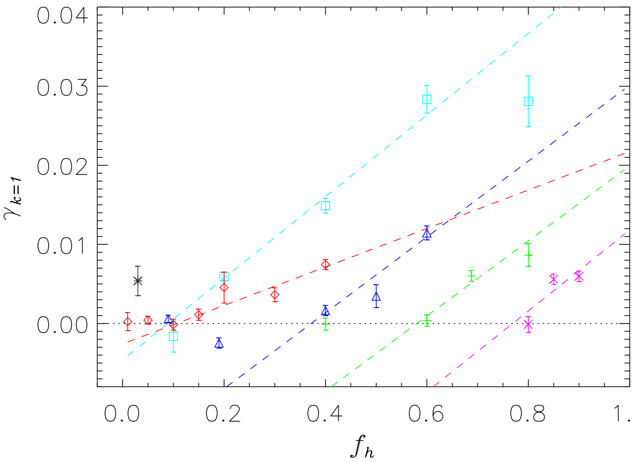

FIG. 3. Growth rate $\gamma_{k=1}$ of $E_b(k = 1)$ versus fractional helicity. From Table I, × (pink, $k_F = 2$), + (green, $k_F = 3$), □ (cyan, $k_F = 4$), △ (blue, $k_F = 5$), ◇ (red, $k_F = 6$), grey, $*$ ($k_F = 8$) and least-squares linear fits (dashed).

uration for the $k = 6$ mode. The $k = 1$ mode accounts for nearly 10% of E_b by 100τ and the growth rate slows, but has not fully saturated by 300τ. The growth rate of magnetic energy at $k = 1$ during the SSD phase is nearly the same for all of our runs, and is insensitive to f_h, R_M, and k_F. Sensitivity to f_h emerges once the SSD regime ends.

The $\gamma_{k=1}$ growth rates (for $E_b(k = 1)$) that immediately follow the SSD phase (see Table I) are shown in Fig. 3. This LSD growth regime occurs only when $f_h > f_{h,C}$; the LSD growth rate varies linearly with f_h for a fixed k_F/k_{min} ($\alpha \propto H_v \propto f_h$). Least-squares fits are dashed lines in Fig. 3 (the y-intercept, $\beta \sim (k_{min}/k_F)^{2.2}$). The short exponential growth phase of 4-80 makes for an inaccurate measure of $\gamma_{k=1}$; it is thus excluded from the fit. As k_F/k_{min} increases, $f_{h,C}$ decreases.

The LSD exponential growth of $E_b(k = 1)$ for $f_h \geq f_{h,C}$ is accompanied by a $k = 1$ growth of magnetic helicity. Studies of the $k = 1$ growth for $f_h = 1$ in a two-scale approach [14, 15] for a H_R driven dynamo [9] suggest two phases of $k_{min} = 1$ mode growth after the SSD regime: one phase that is largely independent of R_M, and a subsequent R_M dependent asymptotic regime. The former phase has growth consistent with our $\gamma_{k=1}$ phase. In all these runs, $f_{h,C}$ decreases with increasing k_F/k_{min}, as displayed in Fig. 4. For the largest k_F/k_{min} (=8) case, $f_h \sim 3\%$ is sufficient. In Fig. 4, the error bars and $f_{h,C}$ are calculated as follows: The x-intercept from the least-squares linear fits, $\gamma_{k=1} = mf_h + b$ shown in Fig. 3, determine our estimate of $f_{h,C} = -b/m$ for Fig. 4. The

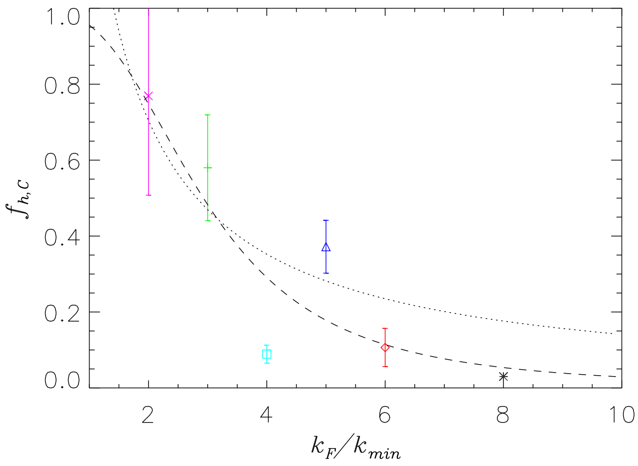

FIG. 4. $f_{h,C}$ from least-squares fits versus k_F/k_{min} (symbols as in Fig. 3). Dashed line is best fit to Eq. (2), giving $C = 0.21$ and $\xi = 0.46$. Dotted line is kinematic MFT prediction $f_{h,C} = \beta k/(|\alpha_0|k_F)$.

$1-\sigma$ uncertainties for b and m are then propagated for $f_{h,C} : \sigma_{f_{h,C}} = b/m\sqrt{(\sigma_b/b)^2 + (\sigma_m/m)^2}$.

Theoretical prediction for $f_{h,C}$- The following prediction for $f_{h,C}$ is based on the principle that LSD helical field growth at $k = k_{min}$ beyond the SSD phase requires helical velocity forcing to overcome the Lorentz force at $k = k_{min}$ at the end of the kinematic SSD phase. For that time, we assume the magnetic energy at $k_{min} < k_F$ to be $B^2_{min} \sim B^2_F(k_{min}/k_F)^{\xi}$, where B_F is the magnetic field at k_F, and $\xi - 1$ is the slope of the magnetic energy spectrum on a log-log plot. The associated Lorentz force is then $M_{nh}(f_h)B^2_F k_F(k_{min}/k_F)^{\xi+1}$, where the function $M_{nh}(f_h) < 1$ accounts for the contribution from only non-helical magnetic energy.

The available helical velocity forcing that must overcome this Lorentz force is only a fraction of the helical forcing at $k = k_F$: At early times when magnetic helicity is nearly conserved, the forcing not only sources magnetic helicity at $k = k_{min}$ but also an oppositely signed, equal in magnitude, magnetic helicity at $k = k_{ss} \geq k_F$. The associated ratio of helical magnetic energy growth at k_{min} to that at k_{ss} is then $\sim k_{min}/k_{ss} < 1$. The helical force that needs to exceed the Lorentz force at k_{min} to initiate growth is thus $\sim K_h(f_h)v^2_{rms}k_F(k_{min}/k_{ss})$, where the function $K_h(f_h) < 1$ accounts for only kinetic helical forcing.

Balancing the aforementioned forces assuming $K_h/M_{nh} = R_h(f_h)$ (which is consistent with our data), and assuming $f_h = f_{h,C}$, then gives

$$f_{h,C} = \frac{1}{1 + C^2(k_F/k_{min})^{2\xi+2}}, \tag{2}$$

where $C \equiv (k_{min}v^2_{rms})/(k_{ss}B^2_F) \sim k_{min}/k_{ss}$. Figure 4 shows the data and the best fit using Eq. (2); $\xi = 0.46 \approx 1/2$ is found. This yields the prediction, $f_{h,C} \sim (k_F/k_{min})^{-3}$ as $k_F/k_{min} \to \infty$. Note that taking the limit of infinite scale separation, we have a LSD with zero helicity (but only fluctuations, as in [21]).

The theory above, which considers the Lorentz force backreaction from the large scale field, can be contrasted with the prediction from the purely kinematic theory of the standard α^2 dynamo which does not include any Lorentz forces. Using the formula presented in the introduction for the growth rate at k_{min}, and the definition of f_h, the critical fractional helicity for the kinematic theory would be $f_{h,C} = \beta k_{min}/(|\alpha_0|k_f)$ where $\alpha_0 \equiv \alpha/f_h$. This formula is shown as the dotted line in Fig. 4 and does not fit the data very well, highlighting the importance of including the Lorentz force. This does not imply the kinematic theory is irrelevant however. For values of $f_h >> f_{h,C}$ the kinematic theory should be applicable to estimating the early time growth rate because the driving helicity overwhelms the backreaction associated with the weak large scale field produced by the SSD in that regime.

Discussion of LSD growth and saturation-At large R_M, SSD action produces field at all scales, potentially precluding a scale separation between the mean magnetic field and velocity fluctuations (an essential assumption to derive α^2 MFT) [22]. The SSD magnetic energy spectrum at scales above the forcing scale produces less magnetic energy the larger the scale [5]. At large enough scales, the magnetic energy production from the SSD will be negligible, and scale separation becomes a meaningful concept (see thin red/light gray, solid line in Fig. 1). This helps justify the mean field approach to LSDs.

In the mean field, two-scale approach, once the small scale magnetic helicity has grown as a result of magnetic helicity conservation to be large enough such that the associated small scale current helicity backreacts on the driving kinetic helicity, the α^2 dynamo eventually slows to R_M-dependent growth rates and ultimately saturates completely. Previous studies have typically focused on the $f_h = 1$ case [14, 15]. In this paper, we have not run enough simulations long enough to determine how strong the large scale field gets before its evolution reaches the R_M dependent regime. However, if cases with fractional helicity $f_{h,C} < f_h < 1$ saturate by direct analogy to the $f_h = 1$ cases studied in previous work, then the value of the large scale magnetic energy reached just before the R_M dependent regime emerges would be expected to be simply proportional to an extra factor of f_h, namely $\overline{B}^2 \sim f_h(k_1/k_f)\langle U^2_{rms}\rangle$. Similarly, for asymptotically saturated steady state at very late times, we would expect $\overline{B}^2 \sim f_h(k_f/k_1)\langle U^2_{rms}\rangle$. Note that in the $f_h = 1$ case, the latter similarity highlights the fact that that super-equipartition field strengths (with respect to the total kinetic energy) are able to grow by the end of the nonlinear, saturated regime for fully helical α^2 dynamo.

Note however that the R_M dependent regimes of the α^2 dynamo are largely irrelevant for astrophysical objects which have such large R_M that something else probably happens before these regimes are reached. Open boundaries and helicity fluxes are ingredients that have to be considered in realistic systems. In addition, real astrophysical dynamos have large scale shear, which amplifies the total large scale field beyond its purely helical value. More work is needed to determine the strength of the large scale fields produced by fractionally helical LSDs.

Conclusion- Only a minuscule amount of fractional helicity is required for LSD action at even modest astrophysically relevant scale separations. For $f_h > f_{h,C}$, the $k = 1$ field grows and the small scale spectrum steepens (see Fig. 1 and [19]). This may be important because our result that $f_{h,C} \lesssim 3\%$ for $k_F/k_{min} \geq 8$, offers a basic principle for potentially reconciling a disparity between a pile up of small scale magnetic energy in large P_M nonhelical dynamo simulations [6] and Galactic observations [18]. Our results also suggest that large scale separations should be a priority in designing laboratory experiments to measure LSD action [2].

Acknowledgements- Computer time was provided by NCAR, Los Alamos National Laboratory and Max-Planck-Institut für Sonnensystemforschung. NCAR is sponsored by NSF. PDM was supported by grants PIP 11220090100825 and PICT-2007-02211. JPG gratefully acknowledges the support of the U.S. Department of Energy through the LANL/LDRD Program for this work.

[1] R. Beck *et al.*, ARA&A **34**, 155 (1996).
[2] D. Lathrop and C. Forest, Physics Today **64**, 40 (2011).
[3] A. Brandenburg, Space Sci. Rev. **144**, 87 (2009).
[4] E.G. Blackman, Astronomische Nach. **331**, 101 (2010).
[5] A.P. Kazantsev, Sov. Phys. JETP **26**, 1031 (1968).
[6] A.A. Schekochihin *et al.*, ApJ **612** 276 (2004)
[7] A. Brandenburg and K. Subramanian, Phys. Rep. **417**, 1 (2005).
[8] M. Meneguzzi, U. Frisch, and A. Pouquet, Phys. Rev. Lett. **47**, 1060 (1981).
[9] A. Pouquet, U. Frisch, and J. Léorat, J. Fluid Mech. **77**, 321 (1976).
[10] H. Moffatt, *Magnetic field generation in electrically conducting fluids* Cambridge University Press,Cambridge, (1978).
[11] A. Brun, M. Miesch, and J. Toomre, ApJ **614**, 1073 (2004);M. Browning, ApJ **676**, 1262 (2008).
[12] A. Gailitis *et al.*, Rev. Mod. Phys. **74**, 973 (2002);H. Ji and S. Prager, MHD **38**, 191 (2002).
[13] P. Roberts and G. Glatzmaier, Rev. Mod. Phys. **72**, 1081 (2000);F. Busse, Ann. Rev. Fluid Mech. **32**, 383 (2000).
[14] A. Brandenburg, ApJ **550**, 824 (2001).
[15] E. Blackman and G. Field, Phys. Rev. Lett. **89**, 265007 (2002).
[16] N.E.L. Haugen, A. Brandenburg, and W. Dobler, ApJ **597** L141 (2003);–, Phys. Rev. E **70** 016308 (2004).
[17] A.A. Schekochihin *et al.*, ApJ **576**, 806 (2002)
[18] A.H. Minter and S.R. Spangler, ApJ, **458** 194 (1996)
[19] J. Maron and E. Blackman ApJ **566**, L41 (2002).
[20] P. D. Mininni *et al.*, Parallel Computing **37**, 316 (2011).
[21] A. Gilbert, U. Frisch, and A. Pouquet, Geophys. Astrophys. Fluid Dynamics **42**, 151 (1988).
[22] F. Cattaneo and D. Hughes, MNRAS **395**, L48 (2009).